

## Highly sensitive and selective detection of the pyrophosphate anion biomarker under physiological conditions

Guzmán Sánchez,<sup>a</sup> David Curiel,<sup>a</sup> Witold Tatkiewicz,<sup>b</sup> Imma Ratera,<sup>b</sup> Alberto Tárraga,<sup>a</sup> Jaume Veciana,<sup>\*b</sup> and Pedro Molina<sup>\*a</sup>

### ELECTRONIC SUPPLEMENTARY INFORMATION

|  |    |
|--|----|
| NRM spectra.....   | 2  |
| XPS data.....  | 3  |
| TOF-SIMS data.....   | 4  |
| PM-IRRAS data.....   | 4  |
| SEM and AFM data.....  | 5  |
| SPR titration of 1-decanthiol SAM.....   | 6  |
| SPR titration of <b>1</b> ·SAM in NaCl 0.1 M.....                                | 6  |
| SPR titration of <b>1</b> ·SAM in 20 mM HEPES saline buffer at pH = 7.4.....     | 7  |
| Selectivity of <b>1</b> ·SAM towards anions with three negative charges.....     | 8  |
| Selectivity of <b>1</b> ·SAM towards other phosphate anions.....                 | 9  |
| Regeneration test of <b>1</b> ·SAM in 20 mM HEPES saline buffer at pH = 7.4..... | 9  |
| Synthesis of compound <b>1</b> .....   | 10 |

## NMR spectra of **1**

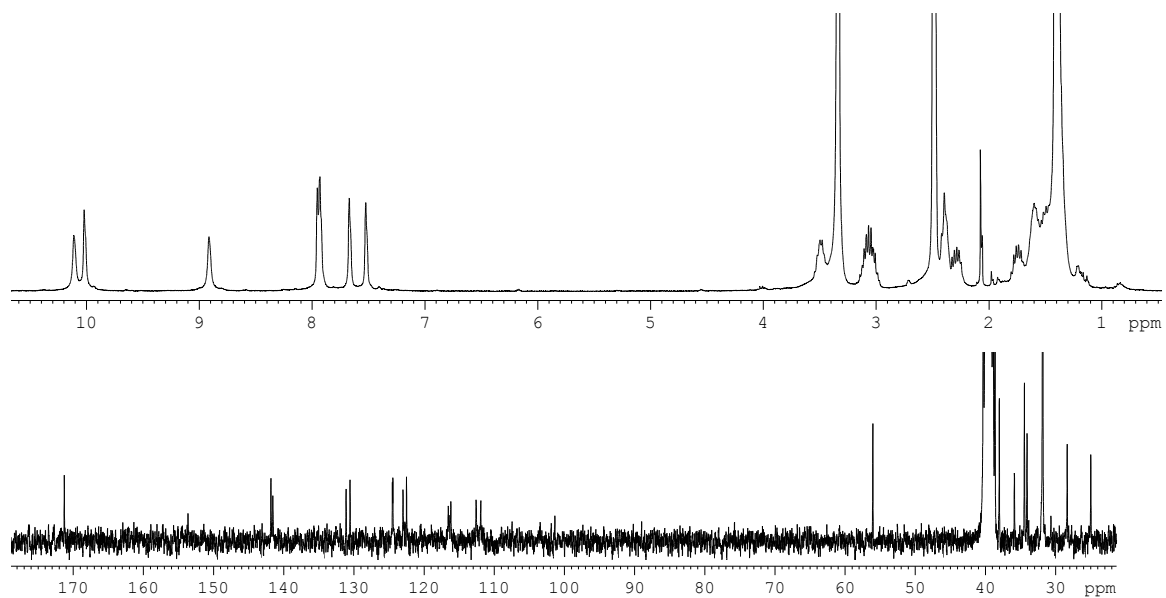


**Figure S1.**  $^1\text{H-NMR}$  (top) and  $^{13}\text{C-NMR}$  (bottom) spectra of **1**.

## Characterization of the monolayers

### XPS data:

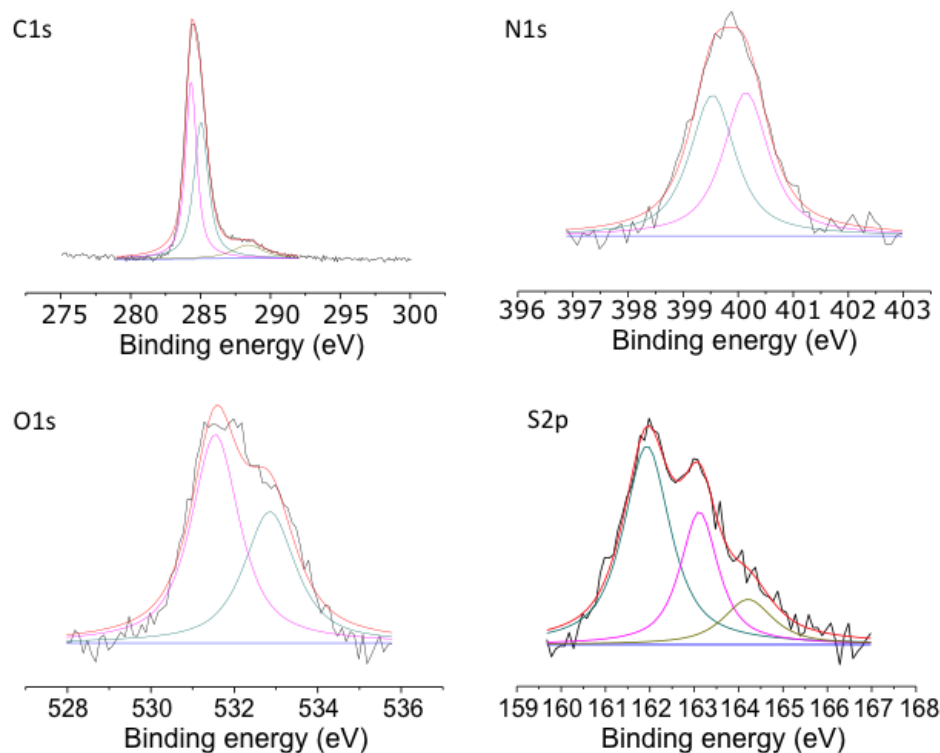


**Figure S2.** Deconvolution of the XPS peaks for each element detected.

**Table S1.** Parameters rendered by the XPS analysis.

| Element/orbital | Bond type                        | Calculated bond energy (eV) | Found bond energy (eV) | Peak area |
|-----------------|----------------------------------|-----------------------------|------------------------|-----------|
| Sulphur 2p      | Bound thiol                      | 162.1                       | 161.93                 | 2628.782  |
|                 | Bound thiol <sup>[a]</sup>       | 162.1                       | 163.11                 | 1419.567  |
|                 | Unbound thiol                    | 164.7                       | 164.21                 | 627.583   |
| Carbon 1s       | C-C, C=C, C-H                    | 284.6                       | 284.32                 | 14431.39  |
|                 | y C-S                            | 286.1                       | 285.03                 | 14606.93  |
|                 | C=O                              | 287.5                       | 288.40                 | 3054.977  |
| Oxygen 1s       | O=C                              | 531.6                       | 531.54                 | 3256.887  |
|                 | O-C                              | 533.2                       | 532.85                 | 4811.747  |
| Nitrogen 1s     | N-C                              | 399.5                       | 399.53                 | 1837.226  |
|                 | N <sup>+</sup> -H <sup>[b]</sup> | 400.2                       | 400.14                 | 1881.968  |

<sup>[a]</sup> Although a bound thiol should exhibit only one band at 162.1 eV, the appearance of two different bands is not uncommon. <sup>[b]</sup> The protonation of NH groups is not infrequent during the XPS measurements.

TOF-SIMS data:

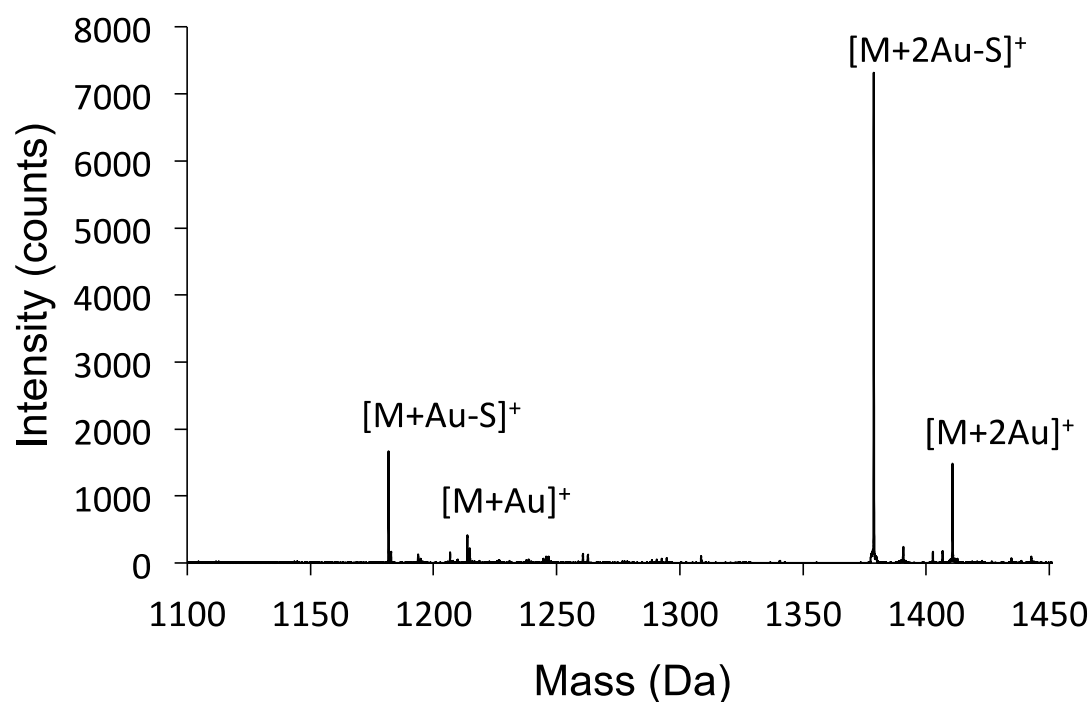


**Figure S3.** Partial TOF-SIMS spectrum with lateral resolution (positive ionization mode) for a gold substrate functionalized with **1** by means of  $\mu$ CP techniques.

PM-IRRAS data:

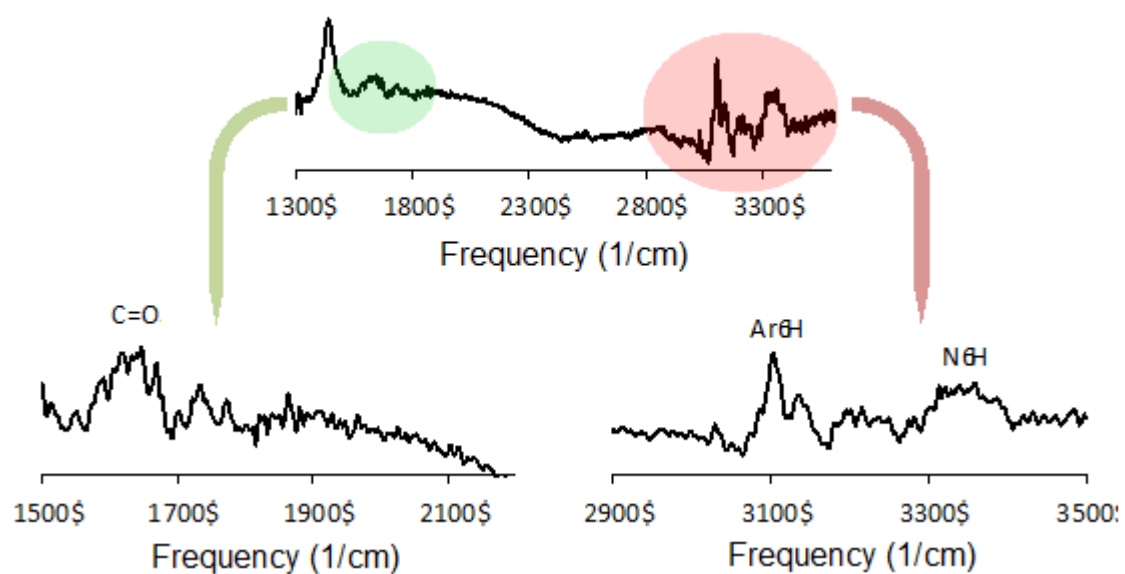


**Figure S4.** PM-IRRAS spectrum. The most relevant bands are shown as insets.

SEM and AFM data:

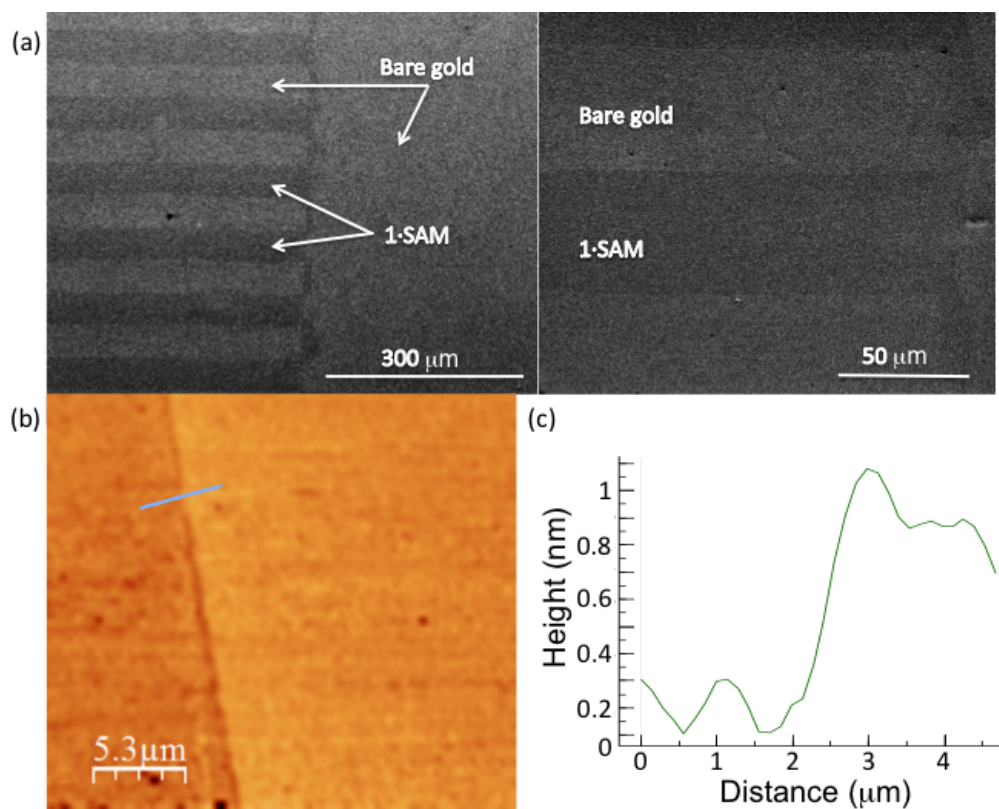


**Figure S5.** SEM and AFM images of printed 1·SAM. a) SEM image of 1·SAM; b) zoom in the border area of the SEM image, b) AFM image of 1·SAM and c) AFM profile of both regions found.

## Surface Plasmon Resonance (SPR) titrations

### 1-Decanethiol SAM:

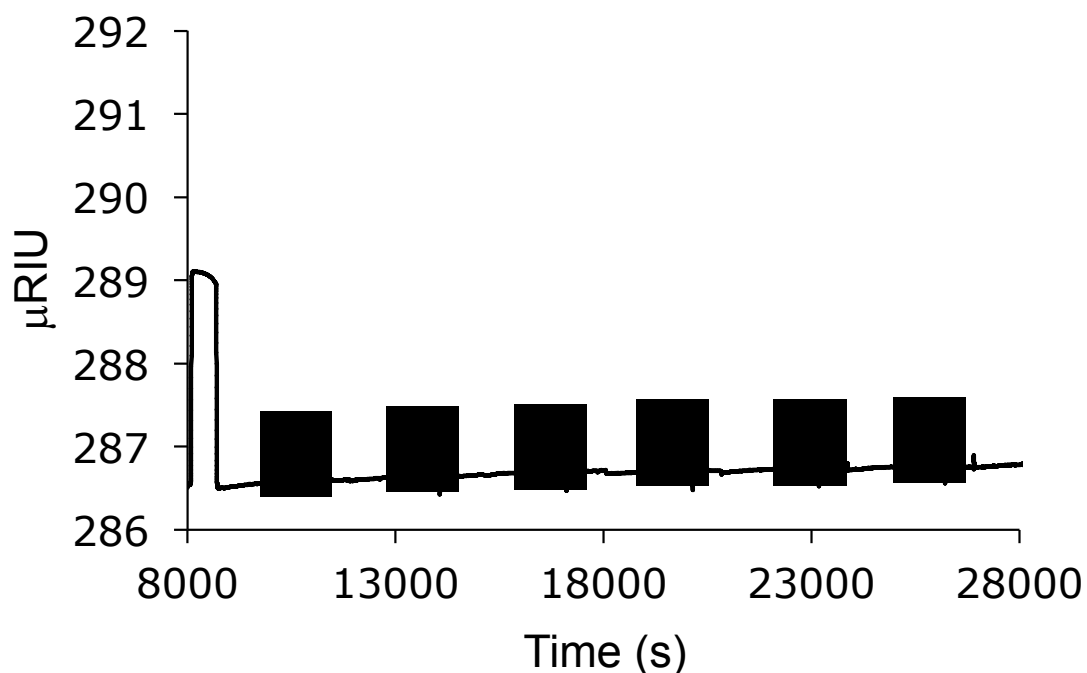


**Figure S6.** SPR sensogram of 1-decanethiol SAM upon addition of different aliquots of  $\text{HP}_2\text{O}_7^{3-}$  anion. An arrow denotes the injection of each concentration of guest.

### 1·SAM in aqueous NaCl 0.1 M:

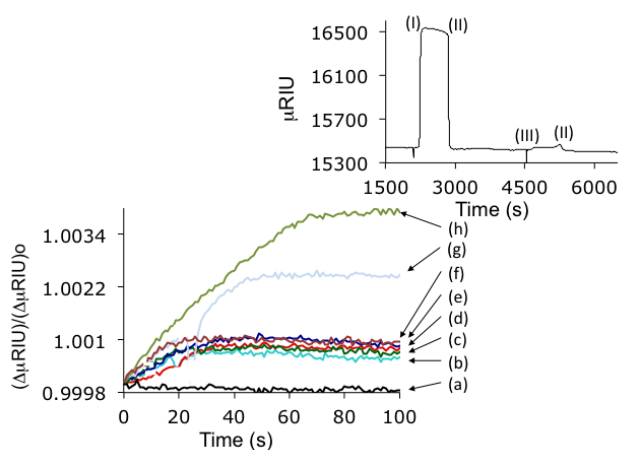


**Figure S7.** Normalized sensogram obtained upon addition of different concentrations of the  $\text{HP}_2\text{O}_7^{3-}$  anion to **1·SAM** in aqueous NaCl 0.1 M. (a) baseline, (b)  $10^{-10}$  M, (c)  $10^{-9}$  M, (d)  $10^{-8}$  M, (e)  $10^{-7}$  M, (f)  $10^{-6}$  M, (g)  $10^{-5}$  M, and (h)  $10^{-4}$  M. Inset: SPR response of a sensing chip functionalized with **1·SAM** upon injection of different concentrations of  $\text{HP}_2\text{O}_7^{3-}$  anion; (I) denotes the injection of a 0.2 M NaCl aqueous

solution as a reference, (II) indicates the washing step with buffer solution (aqueous NaCl 0.1 M in this case) and (III) corresponds to the injection of  $\text{HP}_2\text{O}_7^{3-}$  solutions of different concentrations

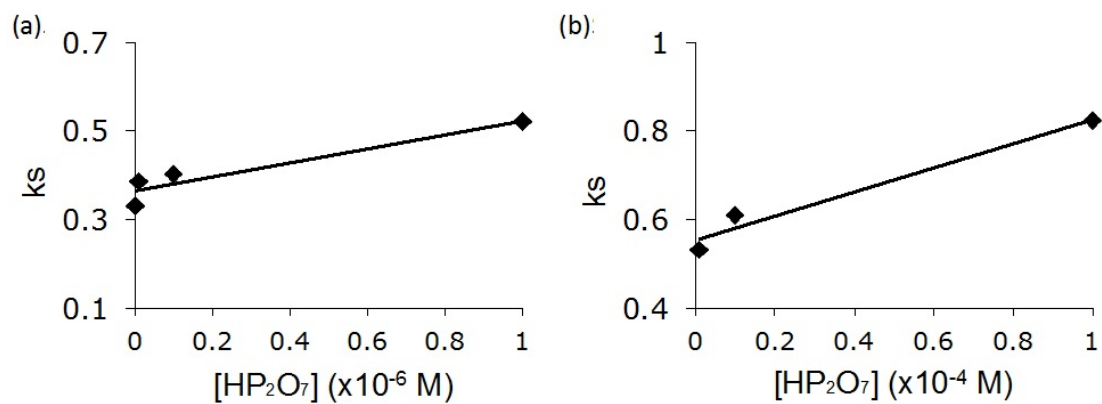


**Figure S8.** Plots of apparent rate constants,  $k_s$ , vs  $[\text{HP}_2\text{O}_7^{3-}]$  at low concentrations (a) and at high concentrations (b).

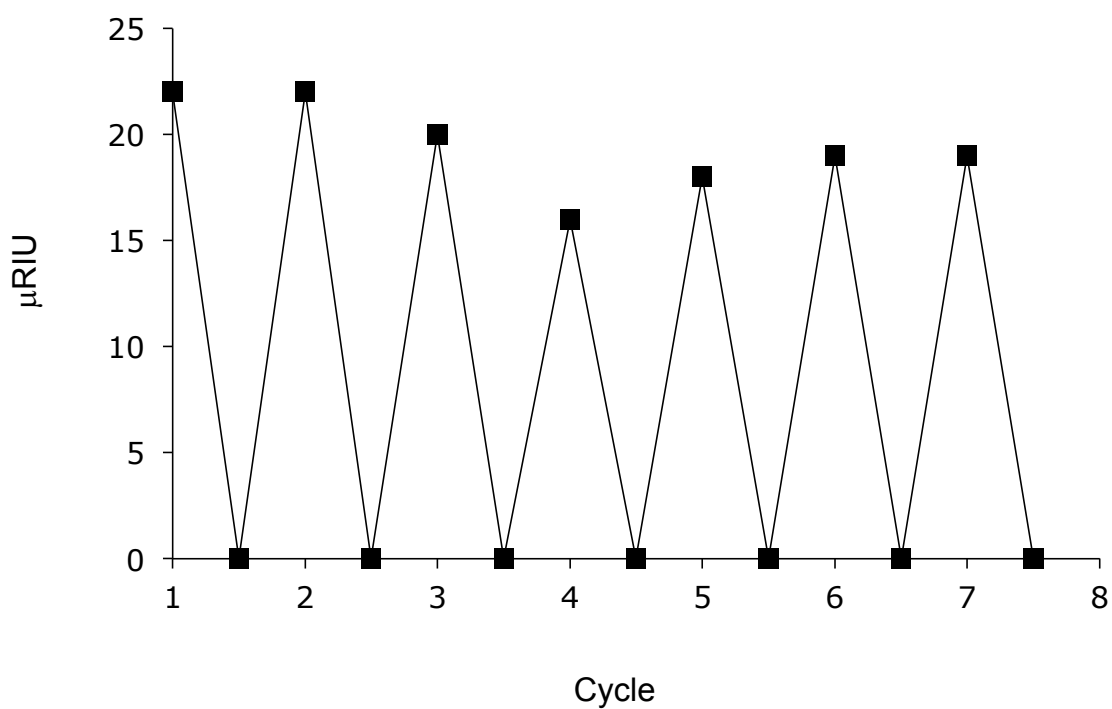


**Figure S9.** Regeneration tests on 1·SAM with  $10^{-9}$  M solutions of  $\text{HP}_2\text{O}_7^{3-}$ .

**1·SAM** in 20 mM HEPES-saline buffer at pH = 7.4:

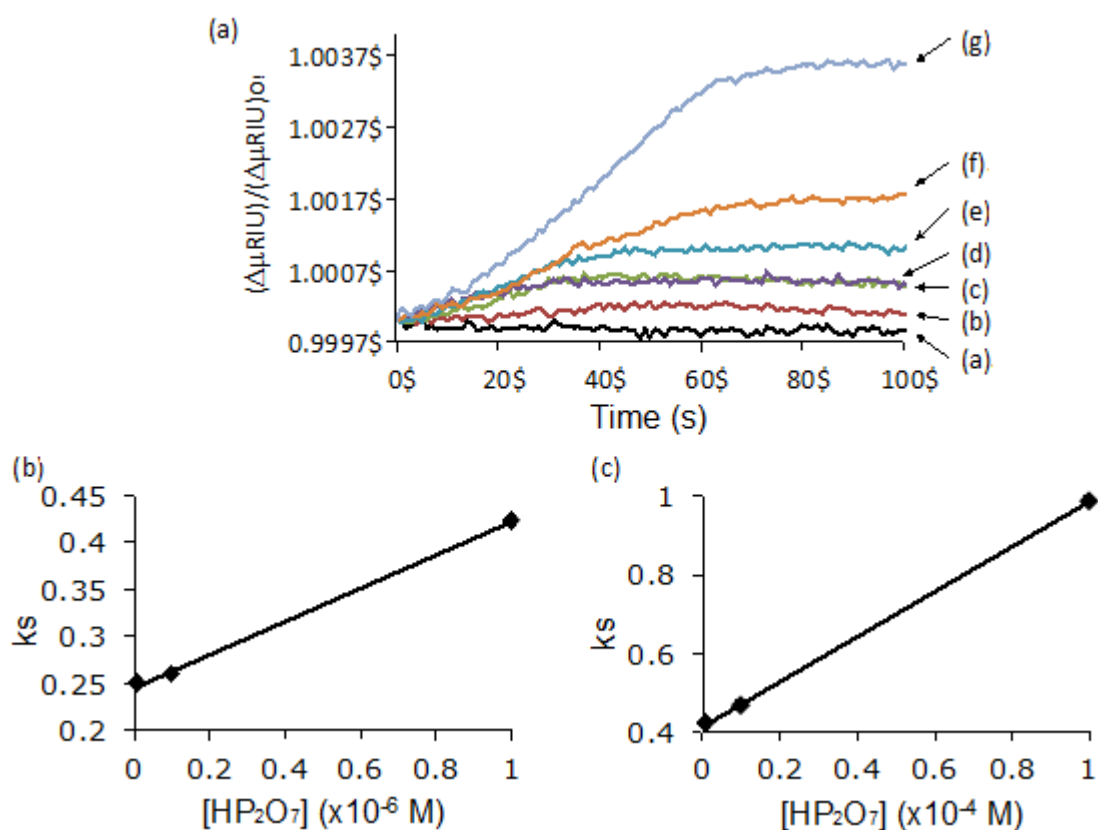


**Figure S10.** (a) Normalized SPR sensogram obtained upon addition of different concentrations of hydrogenpyrophosphate anion to **1·SAM** in 20 mM HEPES-saline buffer (pH = 7.4). (a) baseline, (b)  $[\text{HP}_2\text{O}_7^{3-}] = 10^{-10}$  M, (c)  $[\text{HP}_2\text{O}_7^{3-}] = 10^{-8}$  M, (d)  $[\text{HP}_2\text{O}_7^{3-}] = 10^{-7}$  M, (e)  $[\text{HP}_2\text{O}_7^{3-}] = 10^{-6}$  M, (f)  $[\text{HP}_2\text{O}_7^{3-}] = 10^{-5}$  M and (g)  $[\text{HP}_2\text{O}_7^{3-}] = 10^{-4}$  M. Plots of apparent rate constants,  $k_s$ , vs  $[\text{HP}_2\text{O}_7^{3-}]$  at low concentrations (b) and at high concentrations (c).

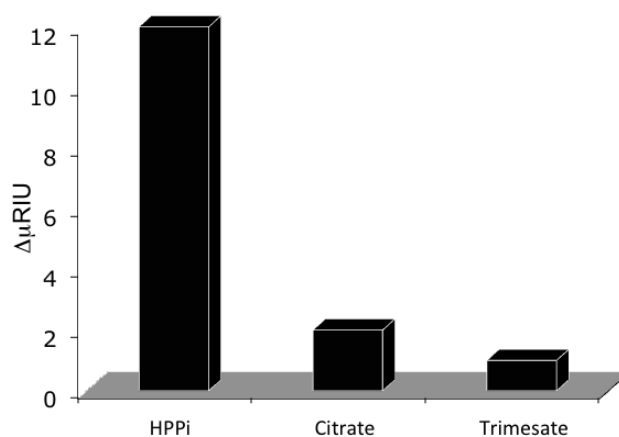


**Figure S11.** Selectivity of **1·SAM** towards trivalent anions. The concentration used was  $10^{-9}$ M for HPPi and  $10^{-7}$ M for the rest of the anions (100-fold excess)



The interfering effects of trivalent citrate and trimesate anions, were tested in 100-fold excess. Surprisingly, the selectivity of the monolayer increased in such physiological media (see Figure S11). Since this environment is more competitive, we can assume that the affinity of **1·SAM** is severely reduced. Nevertheless, while the signal towards hydrogen pyrophosphate is still good, the response showed for the possible competing anions decreased abruptly.

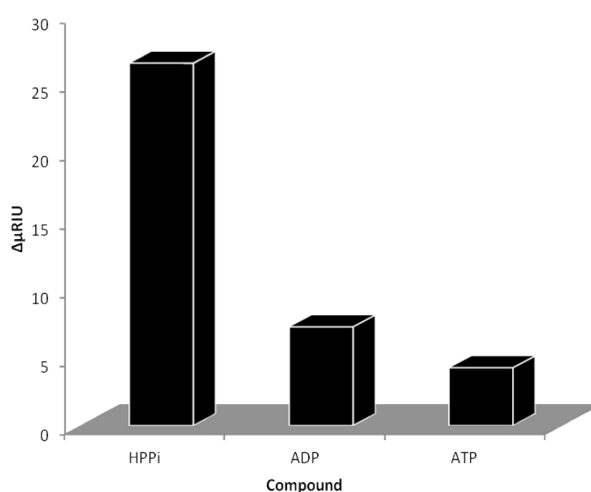


**Figure S12.** Selectivity of **1·SAM** in 20 mM HEPES towards several phosphate anions. The concentration used for all anions were  $10^{-7}$  M.

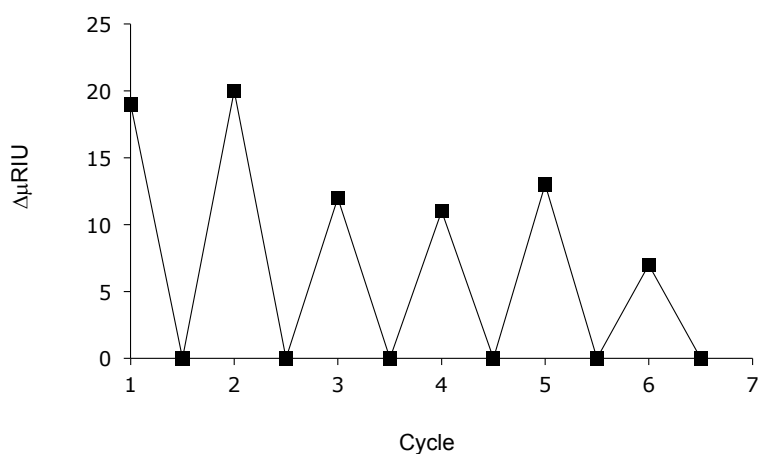


**Figure S13.** Regeneration tests of **1·SAM** in 20 mM HEPES saline buffer using  $[\text{HP}_2\text{O}_7^{3-}] = 10^{-9}$  M.

**Scheme 1. Synthesis of compound 1.**

